

REPORT DOCUMENTATION PAGE					<i>Form Approved</i> OMB No. 0704-0188							
<p>The public reporting burden for this collection of information is estimated to average 1 hour per response, including the time for reviewing instructions, searching existing data sources, gathering and maintaining the data needed, and completing and reviewing the collection of information. Send comments regarding this burden estimate or any other aspect of this collection of information, including suggestions for reducing the burden, to Department of Defense, Washington Headquarters Services, Directorate for Information Operations and Reports (0704-0188), 1215 Jefferson Davis Highway, Suite 1204, Arlington, VA 22202-4302. Respondents should be aware that notwithstanding any other provision of law, no person shall be subject to any penalty for failing to comply with a collection of information if it does not display a currently valid OMB control number.</p> <p>PLEASE DO NOT RETURN YOUR FORM TO THE ABOVE ADDRESS.</p>												
1. REPORT DATE (DD-MM-YYYY)		2. REPORT TYPE New Reprint			3. DATES COVERED (From - To)							
4. TITLE AND SUBTITLE Supramolecular Electrostatic Nanoassemblies for Bacterial Forensics				5a. CONTRACT NUMBER								
				5b. GRANT NUMBER W911NF-09-D-0001								
				5c. PROGRAM ELEMENT NUMBER 611104								
6. AUTHOR(S) Charlene M. Mello, Aidee Duarte, Morris Slutsky, Grady Hanrahan, Guillermo C. Bazan				5d. PROJECT NUMBER								
				5e. TASK NUMBER								
				5f. WORK UNIT NUMBER								
7. PERFORMING ORGANIZATION NAME(S) AND ADDRESS(ES) University of California - Santa Barbara Office of Research The Regents of the University of California Santa Barbara, CA 93106 -2050					8. PERFORMING ORGANIZATION REPORT NUMBER							
9. SPONSORING/MONITORING AGENCY NAME(S) AND ADDRESS(ES) U.S. Army Research Office P.O. Box 12211 Research Triangle Park, NC 27709-2211					10. SPONSOR/MONITOR'S ACRONYM(S) ARO							
					11. SPONSOR/MONITOR'S REPORT NUMBER(S) 55012-LS-ICB.419							
12. DISTRIBUTION/AVAILABILITY STATEMENT Available for public release; distribution unlimited												
13. SUPPLEMENTARY NOTES The views, opinions and/or findings contained in this report are those of the author(s) and should not construed as an official Department of the Army position, policy or decision, unless so designated by other documentation.												
14. ABSTRACT See attached.												
15. SUBJECT TERMS Biosensors, Forensics, Fluorescent probes, FRET, Microbiology, Self-assembly												
16. SECURITY CLASSIFICATION OF: <table border="1" style="width: 100%; border-collapse: collapse;"> <tr> <td style="width: 33%; padding: 2px;">a. REPORT</td> <td style="width: 33%; padding: 2px;">b. ABSTRACT</td> <td style="width: 33%; padding: 2px;">c. THIS PAGE</td> </tr> <tr> <td style="text-align: center; padding: 2px;">UU</td> <td style="text-align: center; padding: 2px;">UU</td> <td style="text-align: center; padding: 2px;">UU</td> </tr> </table>			a. REPORT	b. ABSTRACT	c. THIS PAGE	UU	UU	UU	17. LIMITATION OF ABSTRACT UU		18. NUMBER OF PAGES	
a. REPORT	b. ABSTRACT	c. THIS PAGE										
UU	UU	UU										
					19a. NAME OF RESPONSIBLE PERSON Francis Doyle							
					19b. TELEPHONE NUMBER (Include area code) 805-893-8133							

REPORT DOCUMENTATION PAGE (SF298)
(Continuation Sheet)

Continuation for Block 13

ARO Report Number 55012.419-LS-ICB
Supramolecular Electrostatic Nanoassemblies fo...

Block 13: Supplementary Note

© 2012 . Published in Chemistry - A European Journal, Vol. Ed. 0 18, (3) (2012), (, (3). DoD Components reserve a royalty-free, nonexclusive and irrevocable right to reproduce, publish, or otherwise use the work for Federal purposes, and to authroize others to do so (DODGARS §32.36). The views, opinions and/or findings contained in this report are those of the author(s) and should not be construed as an official Department of the Army position, policy or decision, unless so designated by other documentation.

Report Title

Supramolecular Electrostatic Nanoassemblies for Bacterial Forensics

ABSTRACT

See attached.

Supramolecular Electrostatic Nanoassemblies for Bacterial Forensics

Aidee Duarte,^[a] Morris Slutsky,^[c] Grady Hanrahan,^{*[b]} Charlene M. Mello,^{*[c]} and Guillermo C. Bazan^{*[a]}

Microbial detection and identification are relevant to medicine, biosecurity, and the supply of food and water.^[1] Recent infections with enterohaemorrhagic *Escherichia coli* (*E. coli*)^[2] highlight the need to quickly identify the origin of the pathogen and thereby minimize the impact of the outbreak. Tracking pathogens by their source and environmental history through genetic, proteomic, and traditional microbiological techniques is known as microbial forensics.^[3] The growth medium, temperature, pH, and related factors affect the membrane lipid composition of a variety of microbes.^[4] For example, lipopolysaccharide (LPS) variations have been observed for pathogens such as *Salmonella anatum*,^[5] *E. coli* O157:H7,^[6] and *Yersinia pestis*.^[7] Protein expression also changes with temperature,^[8] and modern proteomic techniques have explored this relationship.^[9] The techniques described above are useful for understanding detailed adaptations under various growth conditions; however they are not amenable to rapid diagnostic assays as they generally require sophisticated, non-portable equipment and may involve time-consuming sample preparation. Simpler methods of relevance to microbial forensics are therefore desired.

Arrays of fluorescent electrostatic aggregates have been used to identify proteins^[10] and bacteria.^[11] This method employs a cationic conjugated oligomer (FPF) and fluorescein-labeled single-stranded DNAs (ssDNA_x-FAM, in which $x = 1-5$, see Figure 1A for molecular structures). Electrostatic

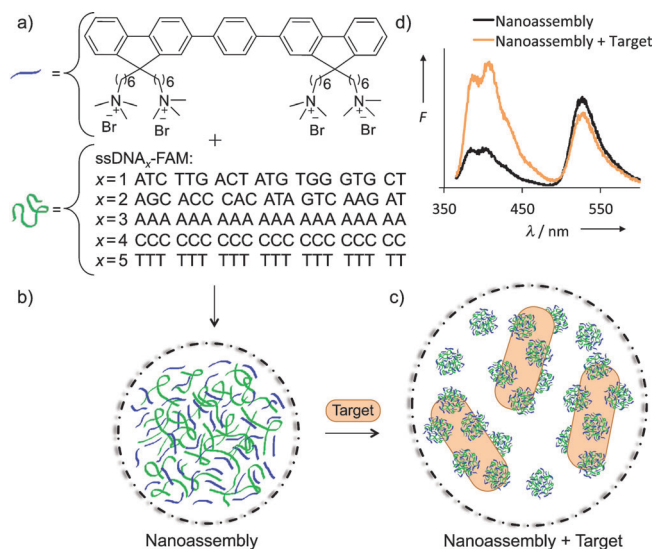


Figure 1. Self-assembly of electrostatic nanoassemblies and their interaction with a target. a) Combination of FPF and ssDNA_x-FAM. b) Generation of the nanoassemblies. c) Non-specific interaction with an analyte. d) PL spectrum of the pure nanoassemblies (black) and the modified spectrum after the introduction of the target, that is protein, cell (orange). Excitation $\lambda = 336$ nm. Drawing is not to scale.

interactions spontaneously bring together the two oppositely charged molecules forming FPF/ssDNA_x-FAM nanoscale aggregates (Figure 1B).^[12] The optical properties of the two partners are such that excitation of FPF is followed by Förster resonance energy transfer (FRET) to FAM. Addition of an analyte alters the non-specific interactions in the FPF/ssDNA_x-FAM nanoassemblies (Figure 1C). Such interactions modify the FPF-FAM distances, and give rise to perturbations in the photoluminescence (PL) spectra (Figure 1D). The collective differential responses from the FPF/ssDNA₁₋₅-FAM array provide a unique signature for the analyte.

Bunz and Rotello have similarly used arrays of gold nanoparticle-conjugated polymer sensors^[13] to detect and identify proteins,^[14] bacteria,^[15] or mammalian normal and cancerous cells.^[16,17] Three strains of *E. coli* were clearly distinguished, suggesting the possibility of differentiating similar biochemical landscapes.^[18]

We therefore hypothesized that the structural changes induced by the selection of growth conditions, in conjunction with the detection method in Figure 1, could be applied within the context of bacterial forensics. Additionally, novel

[a] A. Duarte, Prof. G. C. Bazan
Institute for Collaborative Biotechnologies
Department of Chemistry & Biochemistry
University of California
Santa Barbara, CA 93106 (USA)
Fax: (+1) 805-893-3803
E-mail: bazan@chem.ucsb.edu

[b] Prof. G. Hanrahan
Hugh and Hazel Darling Center for Applied Scientific Computing
Department of Chemistry, California Lutheran University
Thousand Oaks, CA 91360 (USA)
Fax: (+1) 805-493-3392
E-mail: ghanraha@clunet.edu

[c] M. Slutsky, Dr. C. M. Mello
Biosciences and Technology Team
US Army Natick Soldier RDEC
Natick, MA 01760-5020 (USA)
Fax: (+1) 508-999-8451
E-mail: Charlene.mello@us.army.mil

Supporting information for this article is available on the WWW under <http://dx.doi.org/10.1002/chem.201103237>.

computational techniques were employed to examine the influence of experimental variables on the differential response to cells prepared under different growth conditions. As an initial objective we optimized the nanoassembly conditions by focusing on the FPF/ssDNA₂-FAM response toward *E. coli* K12 cells grown in Luria broth (LB) at 37°C. Experimental conditions previously used to differentiate between bacterial species^[11] were used as the starting point and values above and below were explored (Table 1). The

Table 1. Experimental variables and ranges investigated and optimized for differential response.

Buffer concentration [mM]	Charge ratio $R_{+/-}$	FPF concentration [μ M]
3	0.7	1
7	1.0	3
12	1.5	5
17	2.0	7
21	2.3	9

charge ratio, $R_{+/-}$, was calculated by dividing the total number of positive charges from FPF by the total number of negative charges from ssDNA₂-FAM. The spectral response was quantified as δ , as described by Equation (1):

$$\delta = \frac{B_{\text{bac}}}{B_0} + \frac{G_0}{G_{\text{bac}}} \quad (1)$$

in which B_0 and B_{bac} are the integrated spectra between 370 and 450 nm and G_0 and G_{bac} are the integrated spectra between 500 and 590 nm for the control probe ($\text{OD}_{600}=0$) and in the presence of the bacteria ($\text{OD}_{600}=0.05$), respectively. A normalized bacterial optical density was employed to focus on the differences among the cells grown under various conditions.

A central composite experimental design^[19] was first employed to correlate the conditions in Table 1 with experimentally determined δ values and determine variable significance. The latter was determined by using the significance probability for the F -ratio ($\text{Prob}>F$), which is the ratio of the mean square for the variable divided by the mean square for the model error as extracted from the analysis of variance (ANOVA). $\text{Prob}>F$ values less than 0.05 for a variable imply significant influence on the response. This analysis revealed that [FPF] and $R_{+/-}$ were the main significant variables influencing δ , with $\text{Prob}>F$ values <0.001 and 0.0266, respectively. A hybrid, computational neural network model was subsequently employed to predict optimal experimental conditions using the δ response as input (see Figure S1 in the Supporting Information). Neural networks have proved valuable for efficient modeling of experimental variables and complex datasets.^[20] This analysis focused on maximizing differentiating capability and led to the following optimal conditions: 10.5 mM phosphate buffer, $R_{+/-}=1.31$, and [FPF]=4.63 μ M.

The five nanoassemblies were then incorporated with the anticipation of differentiating *E. coli* K12 grown at 37°C in

three different growth media: Luria broth (K12LB), LB agar (K12AG), and nutrient broth (K12NB). Thus, PL spectra were obtained with FPF/ssDNA_x-FAM ($x=1-5$) using the optimal conditions described above and the δ values were calculated. The resulting patterns were subjected to linear discriminant analysis and the canonical score plots are given in Figure 2. The test conditions originally reported^[11]

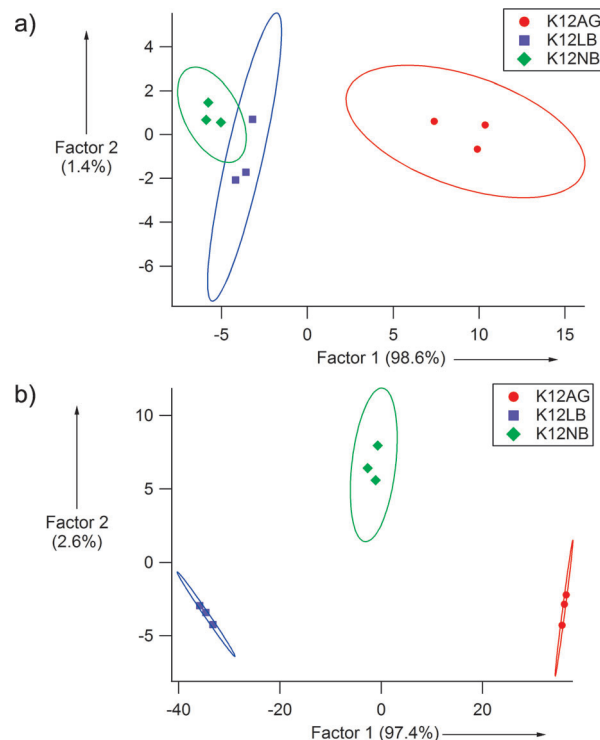


Figure 2. Canonical score plot for the identification of *E. coli* K12 growth conditions obtained by using an array FPF/ssDNA_x-FAM ($x=1-5$) nanoassemblies. a) Using original conditions: 10.0 mM phosphate buffer, $R_{+/-}=1.20$, and [FPF]=4.00 μ M. b) Using optimized conditions: 10.5 mM phosphate buffer, $R_{+/-}=1.31$, and [FPF]=4.63 μ M. Ellipses represent prediction 95 % confidence limits.

had overlapping 95 % prediction ellipses for cells cultured in LB and nutrient broth (Figure 2A). One finds that the optimized experimental conditions allow distinction of the three growth conditions with no overlapping 95 % prediction ellipses (Figure 2B). The smallest squared distance between a point and the nearest ellipse of another group improved from 6 to 1117, a 186-fold increase.

Having established that the experimental conditions generated by the neural network model improved differentiation, we turned our attention to a broader range of growth conditions. Specifically, *E. coli* K12 was cultured on LB agar at 37°C (K12AG), in Luria broth at 25°C (K12LB25), 37°C (K12LB), 42°C (K12LB42), and in nutrient broth at 37°C (K12NB). PL spectra for each of the FPF/ssDNA_x-FAM ($x=1-5$) nanoassemblies are shaded black in Figure 3. Upon *E. coli* K12 introduction, the spectral profiles were uniquely perturbed depending on the media and temperature of growth, leading to distinct PL characteristics with each of the assemblies.

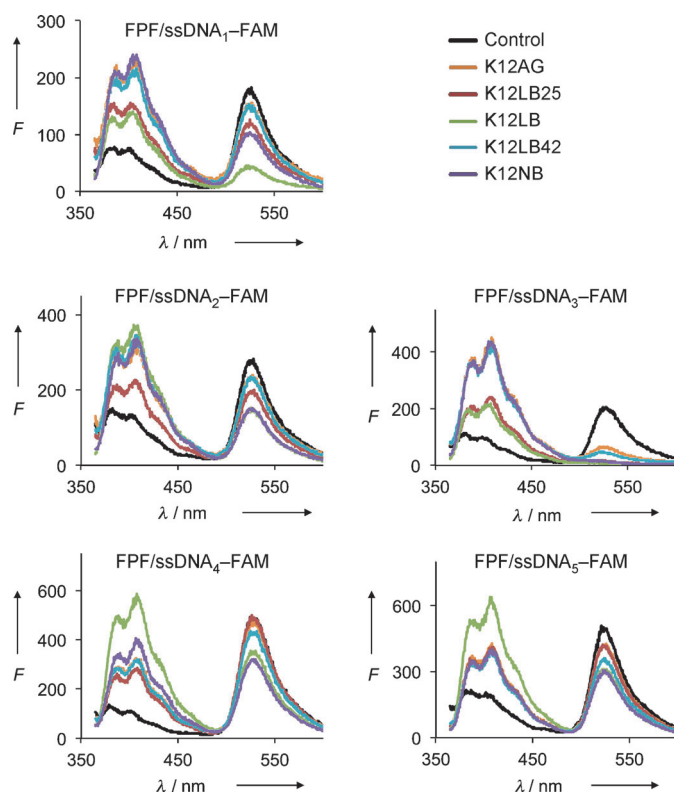


Figure 3. Photoluminescence spectra of FPF/ssDNA_x-FAM ($x=1-5$) nanoassemblies. Traces in black correspond to control experiments, that is $OD_{600}=0$. The modified PL spectra after the introduction of *E. coli* K12, $OD_{600}=0.05$. Excitation $\lambda=336$ nm. Conditions: 10.5 mM phosphate buffer, $R_{+/-}=1.31$, and $[PFF]=4.63$ μ M.

Canonical score plots obtained from the PL spectra in Figure 3 that used the δ response as in Equation (1) failed to be sufficiently different for achieving differentiation. The blue and green spectral components were therefore separated to generate a more complex ten-component response pattern (Figure 4A). Figure 4B shows the corresponding canonical score plot. Bacterial classifications were made on the basis of the shortest Mahalanobis distances from each point to the multivariate mean of each class.^[16] Canonical factor variables 1–4 contained 81.0, 11.4, 6.9, and 0.7% of the variability, respectively. In the canonical score plot, a distinction was present between the cells cultured in LB media at 25°C, LB media at 37°C, and nutrient broth at 37°C, whereas the confidence ellipses of cells cultured on LB agar at 37°C and LB media at 42°C overlapped. Out of the 30 experimental points, 26 were correctly characterized. The array of nanoassemblies were able to clearly identify cells cultured in three different growth conditions, while it failed to distinguish cells grown on LB agar at 37°C and in LB at 42°C.

The nanoassembly array platform was next challenged with a different strain, the food pathogen *E. coli* O157:H7. These experiments were performed in a different laboratory at a different University from those described for *E. coli* K12 to demonstrate reproducibility. Figure 5A shows the ten component response pattern for *E. coli* O157:H7 cul-

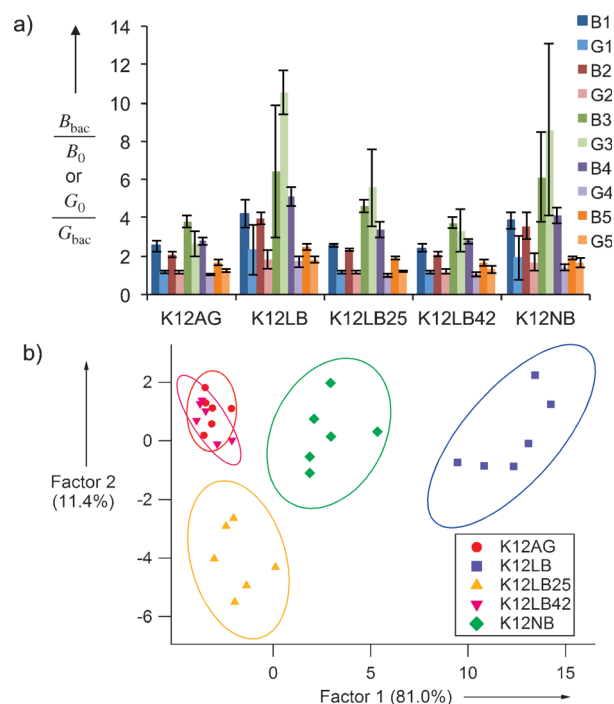


Figure 4. Array identification of *E. coli* K12 growth conditions. a) Response pattern for *E. coli* K12, $OD_{600}=0.05$, in which B and G represent B_{bac}/B_0 , G_b/G_{bac} , respectively, and the number corresponds to x in FPF/ssDNA_x-FAM. Error bars represent the standard deviation of the data. b) Canonical score plot of the response pattern. Ellipses represent the prediction 95% confidence limits. Conditions: 10.5 mM phosphate buffer, $R_{+/-}=1.31$, and $[PFF]=4.63$ μ M.

tured on LB agar plates at 37°C (O157AG), in Luria broth at 25°C (O157LB25), 37°C (O157LB), 42°C (O157LB42), and in nutrient broth at 37°C (O157NB). Figure 5B presents the resulting canonical score plot. Canonical factor variables 1–4 for the classification contained 50.9, 38.7, 10.0, and 0.4% of the variability, respectively. The *E. coli* O157:H7 bacteria groups showed distinct clusters in the canonical score plot with the exception of LB-grown and nutrient broth-grown cells at 37°C for which the 95% prediction ellipses overlapped. All of the *E. coli* O157:H7 growth conditions were correctly classified. Furthermore, each of these measurements included two independently grown cell batches for each growth condition. Substantial overlap between 95% confidence ellipses of each growth condition was observed (Figure S2 in the Supporting Information). This set of results indicates that the spectral response of the FPF/ssDNA_x-FAM assemblies reproducibly reports on the growth conditions of the bacteria.

To summarize, simple to prepare electrostatic nanoassemblies that comprise the conjugated oligoelectrolyte FPF and FAM-labeled ssDNA have sufficiently different structural attributes and spectral responses for obtaining information on the growth characteristics of bacteria. The data in Figure 4 and 5 validate that it is possible to use the composite array response of the nanoassemblies to define profiles that are characteristic to the history of the microbe. This work also demonstrates the importance of optimizing the

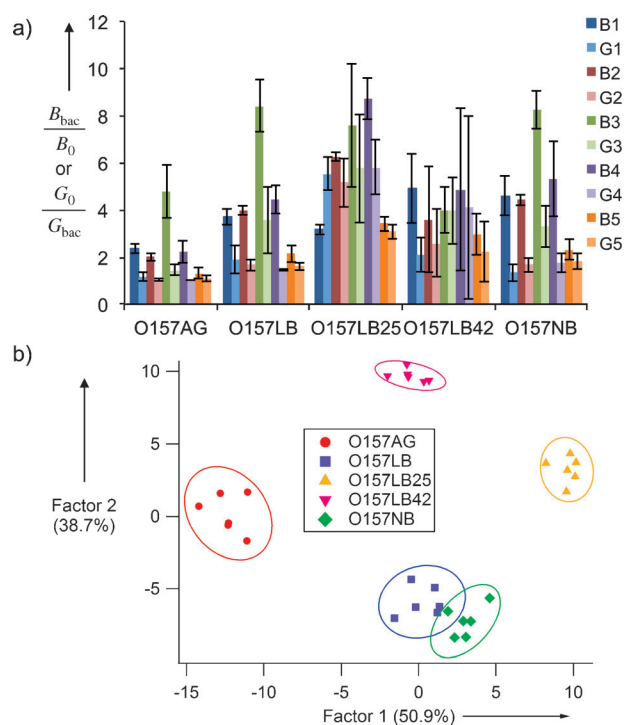


Figure 5. Array identification of *E. coli* O157:H7, $OD_{600}=0.05$, grown under different conditions. a) Response pattern in which B and G represent B_{bac}/B_0 , G_0/G_{bac} , respectively, and the number corresponds to x in FPF/ssDNA_x-FAM. Error bars represent the standard deviation of the data. b) Canonical score plot of the response pattern. Ellipses represent the prediction 95% confidence limits. Conditions: 10.5 mM phosphate buffer, $R_{+/-}=1.31$, and $[FPF]=4.63 \mu\text{M}$.

differentiation conditions and the utility of neural networks for achieving this goal without the need to examine all possible conditions experimentally. It is also worth highlighting that the work has been carried out in two independent laboratories to demonstrate the reproducibility of the results. Altogether, these findings demonstrate a simple to use methodology whereby supramolecular optical systems with slightly different structural attributes can be used as a new tool in bacterial forensics.

Acknowledgements

The authors thank Dr. Wallace Buchholz for inspiration and helpful discussions. We are grateful to the Institute for Collaborative Biotechnologies for financial support. A.D. thanks the Ford Foundation and the National Research Council of the National Academies.

Keywords: biosensors • forensics • fluorescent probes • FRET • microbiology • self-assembly

- [1] a) R. Dalton, *Nature* **2001**, *413*, 657–658; b) A. R. Hoffmaster, C. C. Fitzgerald, E. Ribot, L. W. Mayer, T. Popovic, *Emerging Infect. Dis.* **2002**, *8*, 1111–1116.
- [2] WHO/Europe | Outbreaks of *E. coli* O104:H4 infection: update 29. <http://www.euro.who.int/en/what-we-do/health-topics/emergencies/>

- international-health-regulations/ehc-outbreak-in-germany (accessed July 2011).
- [3] B. Budowle, R. Murch, R. Chakraborty, *Int. J. Leg. Med.* **2005**, *119*, 317–330.
- [4] a) M. Suutari, S. Laakso, *Crit. Rev. Microbiol.* **1994**, *20*, 285–328; b) H. G. Yuk, D. L. Marshall, *Appl. Environ. Microbiol.* **2004**, *70*, 3500–3505; c) H. G. Yuk, D. L. Marshall, *Appl. Environ. Microbiol.* **2003**, *69*, 5115–5119; d) H. J. Chung, W. Bang, M. A. Drake, *Compr. Rev. Food Sci. Food Saf.* **2006**, *5*, 52–64; e) G. H. Joyce, R. K. Hammond, D. C. White, *J. Bacteriol.* **1970**, *104*, 323–330; f) M. E. Guenzoni, R. Lanciotti, P. S. Cocconcelli, *Microbiology-Sgm* **2001**, *147*, 2255–2264; g) C. J. Ehrhardt, V. Chu, T. Brown, T. L. Simmons, B. K. Swan, J. Bannan, J. M. Robertson, *Appl. Environ. Microbiol.* **2010**, *76*, 1902–1912.
- [5] M. McConnell, A. Wright, *J. Bacteriol.* **1979**, *137*, 746–751.
- [6] K. L. Dodds, M. B. Perry, I. J. McDonald, *Can. J. Microbiol.* **1987**, *33*, 452–458.
- [7] a) H. A. Colburn, D. S. Wunschel, K. C. Antolick, A. M. Melville, N. B. Valentine, *J. Microbiol. Methods* **2011**, *85*, 183–189; b) Y. A. Knirel, B. Lindner, E. V. Vinogradov, N. A. Kocharova, S. N. Senchenkova, R. Z. Shaikhutdinova, S. V. Dentovskaya, N. K. Fursova, I. V. Bakhteeva, G. M. Titareva, S. V. Balakhonov, O. Holst, T. A. Gremyakova, G. B. Pier, A. P. Anisimov, *Biochemistry* **2005**, *44*, 1731–1743; c) D. S. Wunschel, H. A. Colburn, A. Fox, K. F. Fox, W. M. Harley, J. H. Wahl, K. L. Wahl, *J. Microbiol. Methods* **2008**, *74*, 57–63.
- [8] S. L. Herendeen, R. A. VanBogelen, F. C. Neidhardt, *J. Bacteriol.* **1979**, *139*, 185–194.
- [9] a) Y. H. Kim, K. Y. Han, K. Lee, J. Lee, *Appl. Microbiol. Biotechnol.* **2005**, *68*, 786–793; b) M. P. Molloy, B. R. Herbert, M. B. Slade, T. Rabilloud, A. S. Nouwens, K. L. Williams, A. A. Gooley, *Eur. J. Biochem.* **2000**, *267*, 2871–2881; c) K. Trunk, B. Benkert, N. Quack, R. Munch, M. Scheer, J. Garbe, L. Jansch, M. Trost, J. Wehland, J. Buer, M. Jahn, M. Schobert, D. Jahn, *Environ. Microbiol.* **2010**, *12*, 1719–1733; d) L. M. Smoot, J. C. Smoot, M. R. Graham, G. A. Somerville, D. E. Sturdevant, C. A. L. Migliaccio, G. L. Sylva, J. M. Musser, *Proc. Natl. Acad. Sci. USA* **2001**, *98*, 10416–10421.
- [10] H. Li, G. C. Bazan, *Adv. Mater.* **2009**, *21*, 964–967.
- [11] A. Duarte, A. Chworos, S. F. Flagan, G. Hanrahan, G. C. Bazan, *J. Am. Chem. Soc.* **2010**, *132*, 12562–12564.
- [12] C. Chi, A. Chworos, J. Zhang, A. Mikhailovsky, G. C. Bazan, *Adv. Funct. Mater.* **2008**, *18*, 3606–3612.
- [13] O. R. Miranda, B. Czeran, V. M. Rotello, *Curr. Opin. Chem. Biol.* **2010**, *14*, 728–736.
- [14] a) M. De, S. Rana, H. Akpınar, O. R. Miranda, R. R. Arvizo, U. H. F. Bunz, V. M. Rotello, *Nat. Chem.* **2009**, *1*, 461–465; b) C. C. You, O. R. Miranda, B. Gider, P. S. Ghosh, I.-B. Kim, B. Erdogan, S. A. Krovi, U. H. F. Bunz, V. M. Rotello, *Nat. Nanotechnol.* **2007**, *2*, 318–323.
- [15] R. L. Phillips, O. R. Miranda, C.-C. You, V. M. Rotello, U. H. F. Bunz, *Angew. Chem.* **2008**, *120*, 2628–2632; *Angew. Chem. Int. Ed.* **2008**, *47*, 2590–2594.
- [16] A. Bajaj, O. R. Miranda, I. B. Kim, R. L. Phillips, D. J. Jerry, U. H. F. Bunz, V. M. Rotello, *Proc. Natl. Acad. Sci. USA* **2009**, *106*, 10912–10916.
- [17] A. Bajaj, O. R. Miranda, R. Phillips, I. B. Kim, D. J. Jerry, U. H. F. Bunz, V. M. Rotello, *J. Am. Chem. Soc.* **2010**, *132*, 1018–1022.
- [18] U. H. F. Bunz, V. M. Rotello, *Angew. Chem.* **2010**, *122*, 3338–3350; *Angew. Chem. Int. Ed.* **2010**, *49*, 3268–3279.
- [19] T. Lundstedt, E. Seifert, L. Abramo, B. Thelin, Å. Nyström, J. Petersen, R. Bergman, *Chemom. Intell. Lab. Syst.* **1998**, *42*, 3–40.
- [20] a) G. Hanrahan, *Anal. Chem.* **2010**, *82*, 4307–4313; b) J. Gasteiger, J. Zupan, *Angew. Chem.* **1993**, *105*, 510–536; *Angew. Chem. Int. Ed. Engl.* **1993**, *32*, 503–527; c) M. Holena, T. Cukic, U. Rodemerck, D. Linke, *J. Chem. Inf. Model.* **2008**, *48*, 274–282.

Received: July 13, 2011
Published online: December 9, 2011